Volume 12 Number 2
Journal of Advances in Physics

Study of the Absorptance of Si-gratings and of arrays of SiO2-filled trenches on Si-grating substrate

ILHEM MEZNI, FAOUZI GHMARI
University of Tunis El Manar, Thermal Unit of Radiation, Department of Physics of the Faculty of Sciences of Tunis,Campus Universitaire, El Manar 1, 2092, Tunis, Tunisia
ilhem_fst@yahoo.fr
faouzi.ghmari@ipein.rnu.tn

ABSTRACT

The purpose of this paper is to study the radiative properties of two model structures. The first model (A-1) is a rectangular grating of silicon (Si). The second one (A-2) is obtained from A-1 by filling their trenches by SiO2. These patterned wafers are characterized by three geometrical parameters, the period d, the filling factor φ and the thickness h. To derive and compute the radiative properties we use a rigorous coupled wave analysis (RCWA) method. Our attention is focused on the absorptance of these structures when they are illuminated by a monochromatic plane wave. We investigate the effect of the filling factor on the absorptance versus the direction of the incident wave. At specific angles of incidence the effect of the period is also studied. Besides, the influence of the thickness h on the absorptance is included throughout this work. At the wavelength λ = 632,8nm, we especially show that we can identify several perfect absorber model structures characterized by specific parameters and by accurate angle of incidence. We show that this will be done in both transverse electric (TE) and transverse magnetic (TM) polarization cases.

Keywords

Coupled wave analysis method, radiative properties, transverse electric and transverse magnetic polarizations, gratings and absorptance.

INTRODUCTION

The prediction of the absorptance of nano-structured surfaces has been the subject of many interesting studies. More generally, radiative properties connected with emission reflection and transmission of such structures have engendered a wide interest because of their various areas of application, including diagnostic systems used in semiconductor industry and thermal systems where radiation transport is important [1, 2]. The study of the coherent emission from patterned wafers with nanoscale linewidth has drained much attention for application in thermo photovoltaic procedures and optoelectronics [3-5]. Chen, Zhang et al. have studied the absorptance of patterned wafers of Si, SiO2 and poly-Si versus wavelength, polarization and angle of incidence [6]. They treated the problem of temperature nonuniformity in rapid thermal processing. Let's note that classical approaches of radiative heat transfer are no longer valid at nano-scale and has been revisited according to the geometric length scales of the surfaces [7, 8]. Experimental measurements of radiative properties [5, 9-14] and numerical investigation [6, 15-18] have been carried out. A variety of one or two-dimensional surface gratings or structures tailored on different materials, especially with photonic crystals, has been studied [19-24]. Authors showed some interesting phenomena related to the interaction of electromagnetic waves with surface microstructures having dimensions comparable to the wavelength.

In this paper we derive and then numerically determine the spectral directional absorptance of two types of model structures. A rectangular grating of silicon (Si), A-1, and an array of SiO2-filled trenches formed in Si substrate, A-2. The geometrical parameters of these structures are the period d, the thickness h and the filling factor φ. They are illuminated by a transverse electric (TE or s) or a transverse magnetic (TM or p) monochromatic plane wave. The direction of incidence lies in the plane perpendicular to the grooves of the surface; it is defined by the angle of incidence θ. A schematic physical system is depicted in figure 1. The optical constants, i.e. the refractive index n and the extinction coefficient κ, of Si and SiO2 in the wavelength range used in this work, are taken from references [6] and [25]. The choice of the temperature of these patterned wafers and that of the wavelength range, are dictated by the work of Chen, Zhang et al. [6].

In this paper we, first, focus on the effect of the filling factor φ on the absorptance. We consider structures A-1 and A-2 with the same period $d = 2\,\mu m$ and with thicknesses h equal to 0.1λ, 0.5λ and λ respectively, and an incident wave of the wavelength λ equal to $0.6328\ \mu m$. The two polarization cases, TE and TM, are considered. The effect, of filling the tranches of A-1 by SiO2 on the behavior of the absorptance versus the filling factor φ, will be widely investigated. At our humble knowledge this study has not been published before for these structures. However, as we will see in section 3 this study leads to some interesting results. Here, let's, only, note that the effect of φ on the absorptance of the structure versus the angle of incidence strongly depends on the thickness h, and obviously on the polarization.

We, second, focus on the influence of the period d on the absorptance. Since, the common and most used filling factor in the literature dealing with such structures (and gratings) made of one or several materials, is $\varphi = 0.5$, we consider structures A-1 and A-2 with this same value of the filling factor. But we vary the period d from 0.1λ to 20λ, and consider thicknesses h equal to 0.1λ, 0.5λ and λ respectively. The angles of incidence are $\theta = 1°$ and $\theta = 60°$; and the wavelength

ISSN 2347-3487
Volume 12 Number 2
Journal of Advances in Physics

λ of the incident wave is again equal to $0.6328\ \mu m$. The two polarization cases are also considered. Here we especially aim to identify some well defined structures which act as nearly perfect absorber, namely with absorptance greater than 0.95.

In this work the absorptance is derived from a Rigorous Coupled Wave Analysis (RCWA) method [6, 26-31]. This choice is dictated by the fact that this method is computationally less expensive than others, such as the surface integral method [32-35], and it is able to handle even deep metallic gratings with any periodic profil [27]. Although, the RCWA method adopted here is widely used, we briefly present in section 2 its main steps leading to the absorptance of the structures. We also briefly expose the associated algorithm that we used for the numerical implementation.

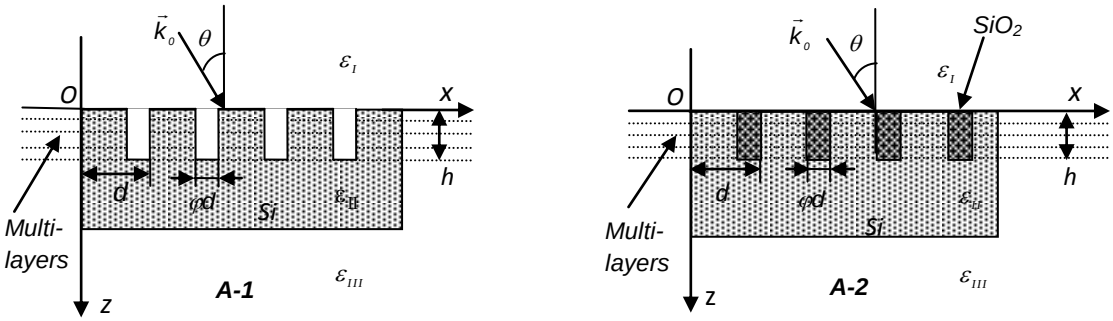

Fig 1:Geometry of the scattering problem.

2. RIGOROUS COUPLED-WAVE ANALYSIS

To determine the absorptance, $\alpha_\lambda'(\theta)$, of the structures considered in this paper, we use a Rigorous Coupled-Wave Analysis (RCWA) method. It particularly leads to calculate the electric-field complex amplitudes of the reflected waves from which we derive the reflected efficiencies. The absorptance is then easily deduced by applying the conservation law of energy at the interface.

The RCWA is based on the electromagnetic theory without any restriction assumptions. Here after we'll present a brief description of the method in the case of a transverse electric polarized incident plane wave.

The first step of the method is to derive the coupled-wave equations inside the grating. For this aim the space is divided into three regions: region I ($z<0$) of incidence, region II of the grating ($0<z<h$) and region III of the substrate ($z>h$). Regions I and III are linear homogenous and isotropic media with constant dielectric permittivity ε_I and ε_{III} respectively. Here after region I is assumed to be free space (or air) with $\varepsilon_I = 1$. However ε_{III} is considered as a complex constant. The modulate region II of the grating is subdivided into M parallel layers with the same thickness, h/M, with M is an integer (Fig. 1). The permittivity of the m^{th} layer, $\varepsilon_m = \varepsilon_m(x, z=z_m)$, is a periodic function of x with period d. Therefore it can be expanded in its Fourier series,

$$\varepsilon_m(x,z_m) = \sum_{\ell=-\infty}^{+\infty} \tilde{\varepsilon}_{m,\ell}\ exp\left(j\,\ell\,K\,x\right), \tag{1a}$$

where $j^2 = -1$, $K = 2\pi/d$ is the magnitude of the grating vector, ℓ is the harmonic index, $\tilde{\varepsilon}_{m,\ell}$ are the complex coefficients of the Fourier series expanding and z_m is the coordinate of the m^{th} layer.

Inside the grating region, the fundamental coupled-wave expansions of the electric field, $E_y(x,z)$ and of the modified magnetic field $h_x(x,z) = \mu_0 c H_x(x,z)$, are given by:

$$E_y(x,z) = \sum_{\ell=-\infty}^{+\infty} E_y^{(\ell)}(z)\,exp(jk_x^{(\ell)}x), \tag{1b}$$

$$h_x(x,z) = \sum_{\ell=-\infty}^{i=+\infty} h_x^{(\ell)}(z)\,exp(jk_x^{(\ell)}x), \tag{1c}$$

Where $k_x^{(\ell)} = k_x^{(0)} + \ell(K/2\pi)$, and $k_x^{(0)} = (2\pi/\lambda)n_0\,sin\theta_\ell$, with θ_ℓ is a discrete refraction angle, n_0 the average refractive index, and ℓ the space harmonic index $\ell = 1,-1,2,-2\ldots,$. Let's outline that the partial fields $E_y^{(\ell)}$ and $h_x^{(\ell)}$ are functions of z, so

that each ℓ does not represent a unique plane wave but it corresponds to an infinite number of plane waves. Farther more these partial fields taken individually do not satisfy the wave equation [40].

Using the expressions (1) of $E_y(x,z)$ and $h_x(x,z)$, and applying the boundaries conditions, Maxwell's equations and the Helmholtz equation one can obtain, after some mathematical manipulations, the following coupled-wave equations,

$$\frac{dE_y^{(\ell)}(z)}{dz} = -jk_0 h_x^{(\ell)}(z), \tag{2a}$$

$$\frac{dh_x^{(\ell)}(z)}{dz} = -j\left\{\frac{\left[k_{z,m}^{\ell}\right]^2}{k_0} E_y^{(\ell)}(z) + k_0 \sum_{k\neq\ell} \tilde{\varepsilon}_{m,\ell-k} E_y^{(\ell)}(z)\right\}, \tag{2b}$$

Where $\left[k_{z,m}^{(\ell)}\right]^2 = k_0^2 \tilde{\varepsilon}_{m,0} - \left[k_x^{(\ell)}\right]^2$, with $k_0 = (2\pi/\lambda)$. Since ℓ is an integer varying between $-\infty$ and $+\infty$, these equations represent an infinite system of first-order differential equations. However, for the numerical calculation we have to retain a finite efficient number N.

The second step is to algebraically resolve the truncated system resulting from system (2). This system can be written in the matrix form, by retaining a finite number N of diffracted orders,

$$\frac{dU}{dz}(z) = [M]U(z), \tag{3}$$

with $0 \le z \le h$, and where U is the 2N vector and $[M]$ is the $2N \times 2N$ matrix both derived from system (2).

The solution of (3) corresponding to the m^{th} slab located between the consecutive coordinates z_m and z_{m+1} ($z_{m+1} > z_m$) will be,

$$U(z_m) = exp\left(-(z_{m+1} - z_m)[M_m]\right)U(z_{m+1}). \tag{4a}$$

Diagonalizing matrix $[M_m]$ we can introduce the matrix $\left[\tilde{P}_m\right]$ build with the eigenvectors of $[M_m]$, and the diagonal matrix $[D_m]$ of the eigenvalues of $[M_m]$, so that, $[M_m] = \left[\tilde{P}_m\right][D_m]\left[\tilde{P}_m\right]^{-1}$ and relation (4a) become,

$$U(z_m) = \left[\tilde{P}_m\right] exp\left(-(z_{m+1} - z_m)[D_m]\right)\left[\tilde{P}_m\right]^{-1} U(z_{m+1}). \tag{4b}$$

The third step is to derive the generalized characteristic matrix. It relates the initial ($z = z_{min}$) and final ($z = z_{max}$) values of electromagnetic field components. For a grating including M substructures, this matrix is expressed as

$$\prod_{m=0}^{M-1}\left[\tilde{P}_m(z_m)\right] exp\left(-(z_{m+1} - z_m)[D_m]\right)\left[\tilde{P}_m(z_{m+1})\right]^{-1} \tag{4c}$$

Now, we introduce forward- and backward-propagating waves in the region I, and we use the Rayleigh field expansions,

$$E_y(x,z) = \sum_{\ell=-\infty}^{\ell=\infty}\left\{f_F^{(\ell)} exp\left[j\left(k_x^{(\ell)}x + k_{Fz}^{(\ell)}z\right)\right] + b_F^{(\ell)} exp\left[j\left(k_x^{(\ell)}x - k_{Fz}^{(\ell)}z\right)\right]\right\}, \tag{5a}$$

$$h_x(x,z) = -\frac{1}{k_0}\sum_{\ell=-\infty}^{\ell=\infty} k_{Fz}^{(\ell)} f_F^{(\ell)} exp\left[j\left(k_x^{(\ell)}x + k_{Fz}^{(\ell)}z\right)\right] + \frac{1}{k_0}\sum_{\ell=-\infty}^{\ell=\infty} k_{Fz}^{(\ell)} b_F^{(\ell)} exp\left[j\left(k_x^{(\ell)}x - k_{Fz}^{(\ell)}z\right)\right], \tag{5b}$$

where $f_F^{(\ell)}$ and $b_F^{(\ell)}$ designate, respectively, the electric-field complex amplitudes of the incident and reflected waves in the region. The k_x^{ℓ} are still defined as indicated above, and $\left[k_{Fz}^{(\ell)}\right]^2 = k_0^2 - \left[k_x^{(\ell)}\right]^2$.

Similar equations can be derived in region III. We denote by $f_L^{(\ell)}$ and $b_L^{(\ell)}$ the complex amplitudes of the forward-and backward-propagating waves in this bottom half-space.

When we note that expansions (1) can also be applied for the upper half-space, it becomes obvious that we have two representations of the electromagnetic field in region I. The first one, in terms of $E_y^{(\ell)}$ and $h_x^{(\ell)}$, is more convenient within the grating. The second one, involving $f_F^{(\ell)}$ and $b_F^{(\ell)}$, is more physics-phenomena intuitive and usually used without the modulate region I. Another important advantage of this second representation is that, it permits an interesting writing of the boundary conditions at $z = z_{min}$. The two representations at this first interface will be connected with the $2N \times 2N$ matrix $[C(z_{min})]$.

Similar derivation will be made at the second interface $z = z_{max}$, introducing $2N \times 2N$ matrix $[C(z_{max})]$, and finally leading to,

$$\begin{bmatrix} \vdots \\ f_F^{(\ell-\gamma)} \\ \vdots \\ b_F^{(\ell-\gamma)} \\ \vdots \end{bmatrix} = [C(z_{min})]^{-1}[\Pi][C(z_{M+1})] \begin{bmatrix} \vdots \\ f_L^{(\ell-\gamma)} \\ \vdots \\ b_L^{(\ell-\gamma)} \\ \vdots \end{bmatrix} \quad (6)$$

with, $[\Pi] = \prod_{m=1}^{M} \left([P_m(z_m)] exp\{-(z_{m+1} - z_m)[D]\} [P_m(z_{m+1})]^{-1} \right)$.

More details concerning this development can be found in reference [26].

Now, let's point that there is only one incident wave in region I and there are no backward propagating waves in region III. Therefore, system (6) is not other than a linear system of 2N equations of 2N unknowns $b_F^{(\ell-\gamma)}$ and $f_L^{(\ell-\gamma)}$. For the numerical simulation we use the algorithm presented in reference [26]. RCWA method for transverse electromagnetic case is similar to that developed above, but with introducing the corrections given by Lifing Li [29, 30].

The directional hemispherical spectral reflectivity (or the reflectance) of the structure, $\rho_\lambda^\cap(\theta)$, due to the spectral directional incident radiation, is defined as the reflected flux into all directions, $'\cap'$, above the surface. Therefore, the reflectance is the summation of the reflected efficiency of all orders. The conservation law of energy leads to the relationship between $\rho_\lambda^\cap(\theta)$ and the spectral absorptance $\alpha_\lambda(\theta)$, as [37]: $\alpha_\lambda(\theta) = 1 - \rho_\lambda^\cap(\theta)$; θ indicates the incident direction.

In this paper, numerical results and physical discussions will be done in terms of the absorptance of the structures. Let's note that the above derivation is taken for any periodic profile surface function of x, with the grating vector defined in the positive x direction. In general, the solution of RCWA converges for a suitable choice of the number M of sub-layers and that of the retained orders N of diffraction. However, since A-1 and A-2 are rectangular gratings a single layer, $M = 1$, is sufficient. The numerical code used in this work is verified by comparison with published results [6, 35].

3. INFLUENCE OF THE FILLING FACTOR ON THE ABSORPTANCE

3.1. Effect of the filling factor on the s-polarized absorptance

a) Rectangular Si-gratings

The left hand-side of figure 2 shows the absorptance of rectangular Si-gratings, $\alpha_\lambda(\theta)$, versus the angle of incidence of a transverse-electric (TE) incoming wave, for different filling-factors φ varying from 0.05 to 0.9.

The absorptance of very thin Si-gratings, of height $h = 0.1\lambda$, is almost not influenced by φ (Fig. 2a). In other words, the fringe-width, φd, of these gratings of period $d = 2000\,nm \approx 3.16\,\lambda$ and $h = 0.1\lambda = 63.28\,nm$, don't affect the absorptance at any angle of incidence. They behave like a flat dielectric surface, of Si, for this wavelength $\lambda = 632.8\,nm$. Let's increase the height, h, of the grating to $h = 0.5\,\lambda = 316.4\,nm$ and then to λ. For these two cases, graphs of $\alpha_\lambda(\theta)$ are shown in figures 2b and 2c respectively. For both cases, changes in the absorptance versus φ occur. This effect depends on the angle of incidence. In fact, when the angle of incidence is smaller than about 30° the absorptance stay fairly uninfluenced by the filling factor φ, however for θ greater than 30° the absorptance varies with φ. So that, we can say that the influence of the width of the rectangular trenches, φd, begins to appear only for relatively deep gratings (here for $h = 0.5\,\lambda$ and $h = 1\,\lambda$) and when the angle of incidence is far away from the normal direction (here for $\theta > 30°$). This can be explained by multiple scattering effects inside the grooves of the grating.

b) Structures A-2

Now let's see how the absorptance is influenced when the trenches of the structures A-1 are filled with SiO_2? This leads to the structures A-2, and we, also, look at the TE polarization case. On the right hand-side of figure 2 the absorptance of numerous structures A-2 is shown, it is significantly changed in comparison with the corresponding one on the left hand-side (case A-1). First, while there is no effect of φ on $\alpha_\lambda(\theta)$ of the Si-gratings A-1 with the thickness $h = 0.1\,\lambda$ (Fig. 2a), we can see from figure 2a' that the influence of φ on the absorptance of the structures A-2, with the same thickness, is clearly manifested. At any angle of incidence, except for $\theta = 90°$, the absorptance is increased as the filling factor φ is increased. Therefore, as the thin SiO_2 film on Si substrate (SiO_2-coated Si) its absorptance is increased. This enhancement of the absorptance is due to the fact that, in general, SiO_2 film behaves as an antireflection coating [33]. Similar behavior of the absorptance for cases A-2 is also observed when the thickness h is increased to $0.5\,\lambda$ and $h = 1\,\lambda$ (Figures *2b'* and *2c'*). The influence of φ on the absorptance of the structures (A-2) is especially important for θ ranging from 30° to 70° when the thickness $h = 1\lambda$. Besides the fact that $\alpha_\lambda(\theta)$ increases with the filling factor φ, it is remarkable

ISSN 2347-3487
Volume 12 Number 2
Journal of Advances in Physics

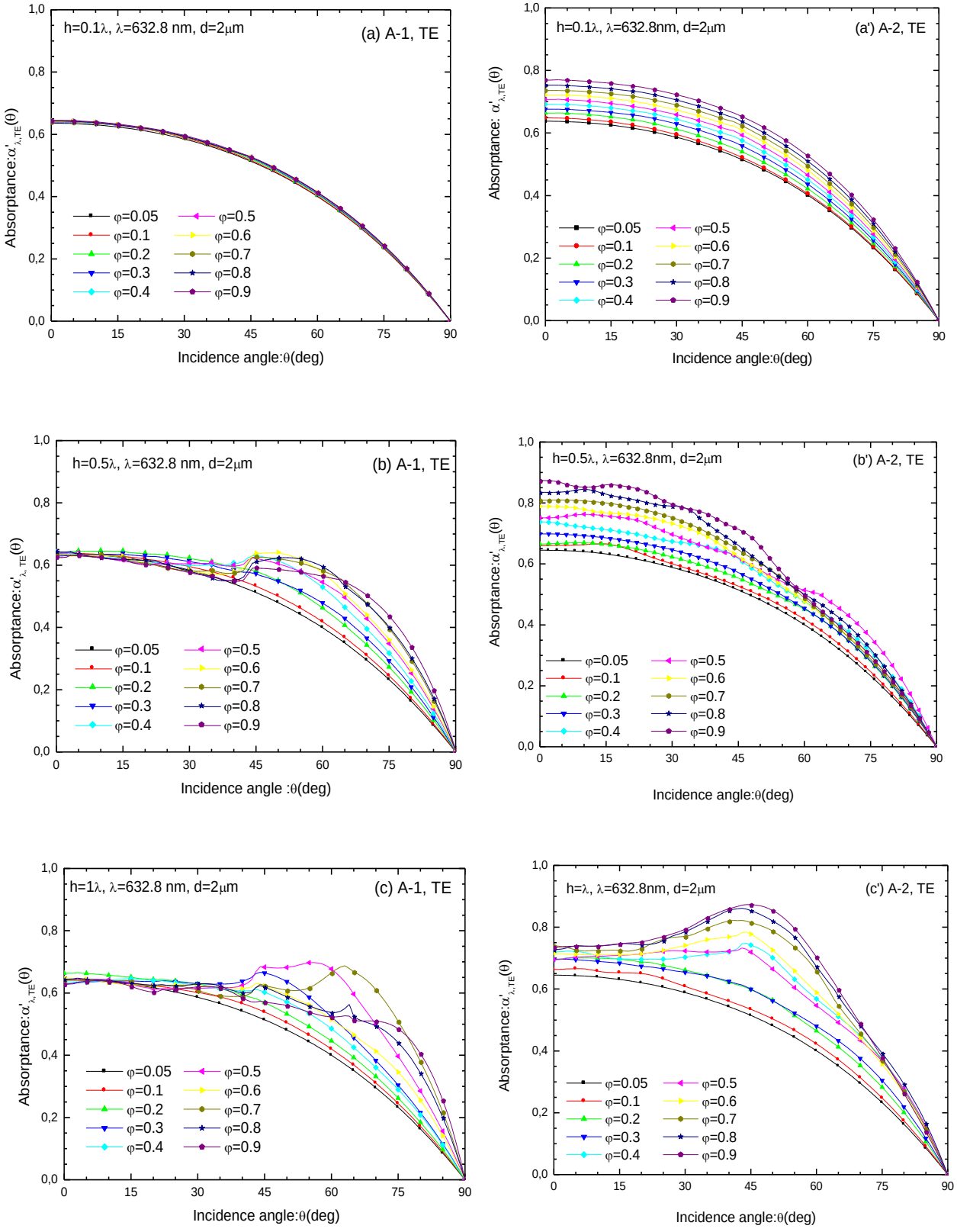

Fig 2. Influence of the filling factor on the absorptance versus the angle of incidence in the transverse electric polarization case. Structures A-1: a) $h = 0.1\lambda$, b) $h = 0.5\lambda$, c) $h = \lambda$. Structures A-2: a') $h = 0.1\lambda$, b') $h = 0.5\lambda$, c') $h = \lambda$.

that it reaches a peak of 0.9 at θ equal to about $45°$ and for $\varphi = 0.9$ (Fig. 2c'); even more a peak of $\alpha_\lambda(\theta)$, versus θ, begins to appear when φ surpasses 0.4. This type of changes of the absorptance versus the angle of incidence is never observed at any value of φ when the height h of the structures (A-2) is either equal to 0.5λ (Fig. 2b') or 0.1λ (Fig. 2a). Let's note that the influence of the filling factor φ on $\alpha_\lambda(\theta)$ persists for θ smaller than 30° (Fig. 2c'), but it is more important for structures of thickness $h = 0.5\lambda$ in this same rang of angles of incidence (Fig. 2b').

3.2. Effect of the filling factor on the p-polarized absorptance

In this subsection we study the effect of the filling factor φ on the spectral absorptance $\alpha_\lambda(\theta)$ versus the angle of incidence in the transverse magnetic polarization case. Numerical results of $\alpha_\lambda(\theta)$ are presented in figures 3 for φ varying from 0.05 to 0.9, for both model structures A-1 and A-2 of the same period $d = 2\mu m$.

The filling factor φ has no effect on the absorptance of a very thin ($h = 0.1\lambda$) rectangular Si-gratings at any angle of incidence (Fig. 3a). But, figure 3a' shows that the absorptance is clearly influenced by φ for structures A-2 with the same thickness $h = 0.1\lambda$ for which the trenches of Si-gratings are filled with SiO_2. The absorptance $\alpha_\lambda(\theta)$ is increasing with the filling factor for θ smaller than about 60°, but it is decreasing when φ is increased for θ greater than 60°. Let's note that in both cases A-1 and A-2 of these very thin structures, the absorptance is increased as θ is increased; it reached its maximum at θ equal to about $75°$. They behave like a dielectric and this maximum is situated to around the Brewster angle [38, 39], for the wavelength $\lambda = 632.8\,nm$, where the reflectance is zero.

The influence of the filling factor φ on the absorptance for the first structure A-1 is clearly observed for the thickness $h = 0.5\lambda$. Figure, 3b, shows that this influence is not discernible for the angles of incidence smaller than $15°$ and for θ equal to about $60°$. The absorptance increases versus the filling factor for θ ranging between $15°$ and $60°$, but it decreases when φ is increased for θ greater than $60°$. This behavior of the absorptance versus the filling factor is shown in figure 3b' for the structure A-2 with the same thickness h equal to 0.5λ; but in this case the dependence of $\alpha_\lambda(\theta)$ on the angle of incidence is not the same as that in the case A-1. In fact $\alpha_\lambda(\theta)$ is the most influenced by φ for θ smaller than $15°$ whereas $\alpha_\lambda(\theta)$ is not affected by φ in this range of θ in the first case.

The filling factor continuous to affect the absorptance of both structures A-1 and A-2 of thickness h equal to the wavelength. This influence of φ on $\alpha_\lambda(\theta)$ is depicted in figures 3c and 3c′. For an angle of incidence close to the normal direction $\theta = 0°$ the absorptance is weakly affected by φ for both model structures. However, the effect of φ on $\alpha_\lambda(\theta)$ becomes more important when θ is near 45°; the absorptance is increasing when φ is increased. This effect is inversed when θ is greater than 60° for the case A-1, and for θ greater than 67.5° in the case A-2.

It is important to point out the existence of an angle of incidence for which there is no influence of the filling factor φ on the absorptance transverse magnetic case. This angle is equal to about $60°$ for Si-gratings (A-1) with thickness $h = 0.5\lambda$, but for Si-gratings filled by SiO_2 (A-2) with the same height this angle is shifted to $65°$. This remarkable angle remains equal to about $60°$ for Si-gratings (A-1) with thickness $h = \lambda$ (Fig. 3c), but again it is shifted to $67.5°$ for the cases A-2 (Fig. 3c′). Let's note that this fact also appears for a very thin structure A-2 with thickness $h = 0.1\lambda$ (Fig. 3a′), for which this angle is equal to $60°$.

4. EFFECT OF THE PERIOD ON THE ABSORPTANCE

4.1. Effect of the period on the s-polarized absorptance at $\theta = 1°$ and $\theta = 60°$

Let us consider structures A-1 and A-2 with the same filling factor $\varphi = 0.5$ and thickness h equal to, 0.1λ, 0.5λ and λ respectively. We study the influence of the period d on the absorptance of these structures. The absorptance $\alpha'_\lambda(d/\lambda)$ of the structures, of the same thickness h, is numerically implemented as a function of the period over the wavelength d/λ. Curves of $\alpha'_\lambda(d/\lambda)$ are depicted in figures 4 in semi-logarithmic coordinates system for the angles of incidence $\theta = 1°$ and $\theta = 60°$. The wavelength is again $\lambda = 632.8\,nm$.

Figure 4a shows that the absorptance at $\theta = 1°$ decreases when the period d of the grating is increased, and tends asymptotically toward 0.63. So that any structure A-1 of period d greater than about 4λ has the same absorptance as the flat surface of Si in this direction. This behavior of the absorptance of these gratings, with thickness $h = 0.1\lambda$, versus the period d, occurs at the angle of incidence $\theta = 60°$ (Fig. 4a). The location of the horizontal asymptote has, obviously, changed, it is now defined by 0.4 which is the absorptance of the plane surface of Si at $\theta = 60°$.

Figure 4a' shows the absorptance in the case A-2. The behavior of the absorptance versus d/λ is similar to that already

ISSN 2347-3487
Volume 12 Number 2
Journal of Advances in Physics

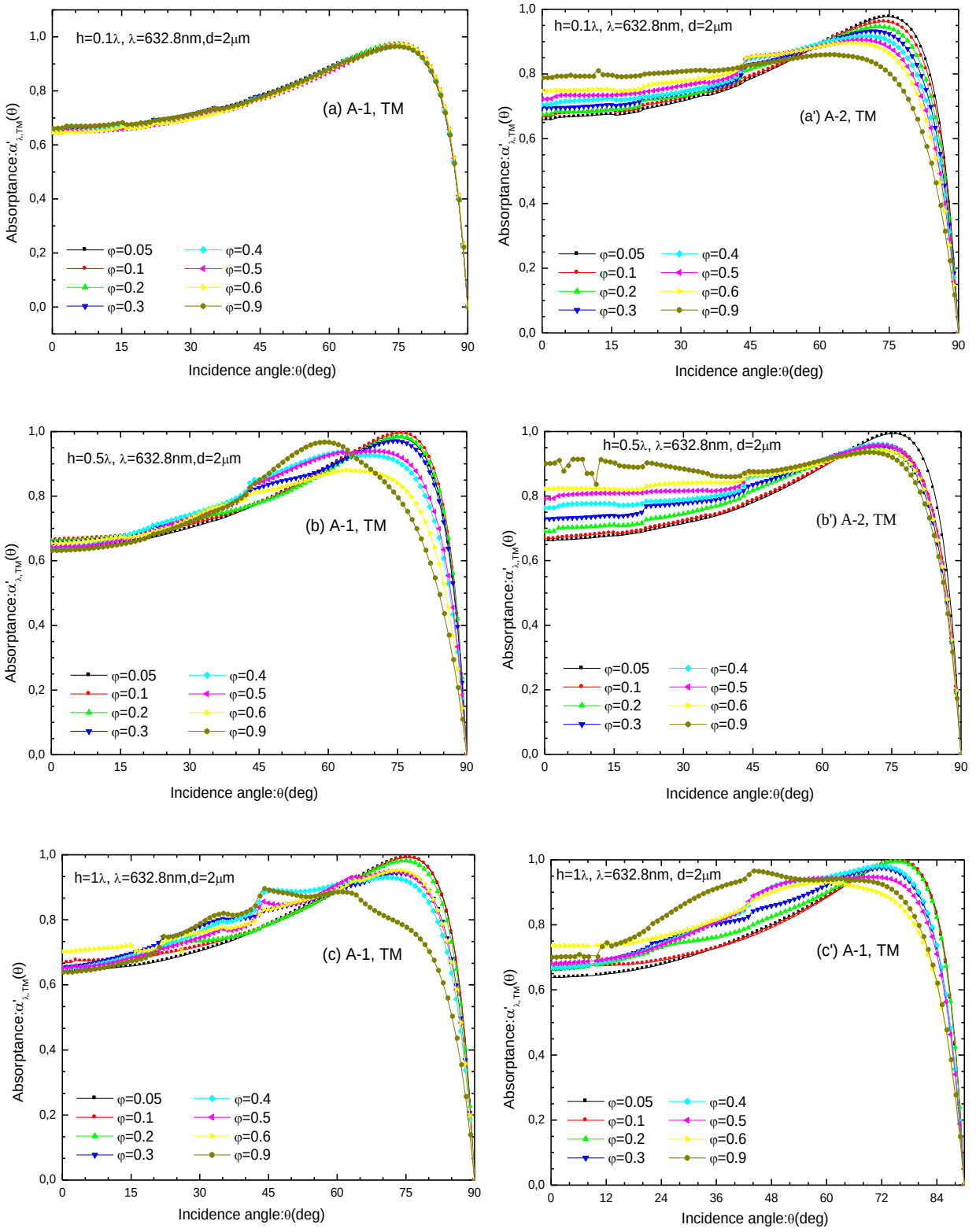

Fig 3. Influence of the filling factor on the absorptance versus the angle of incidence in the transverse magnetic polarization case. Structures A-1: a) $h = 0.1\lambda$, b) $h = 0.5\lambda$, c) $h = \lambda$. Structures A-2: a') $h = 0.1\lambda$, b') $h = 0.5\lambda$ and c') $h = \lambda$.

described for the structures A-1. The horizontal asymptote is, now, located at 0.7 for $\theta = 1°$ and at 0.47 for $\theta = 60°$. The absorptance of these structures A-2 is no longer influenced by the period when d is greater than 2λ. In addition, for d greater than λ, the absorptance of these structures is greater than that of the related Si-gratings. Therefore, the absorptance is increased when the trenches of Si-gratings are filled with SiO_2.

For the gratins A-1, with thickness $h = 0.5\lambda$, figure 4b shows that the s-polarized absorptance at $\theta = 1°$ presents several peaks which are located between $d = 0.4\lambda$ and $d = 2\lambda$. The most remarkable peak is situated at the period $d = 0.92\lambda$ and its magnitude is equal to 0.95. In addition, the absorptance at $\theta = 1°$ becomes constant when d is increased from $d = 4\lambda$ so that there is no effect of the period on the absorptance in this range of d ($d \geq 4\lambda$). For the angle of incidence $\theta = 60°$, the absorptance is similar to that for $\theta = 1°$ (Fig. 4b); but, here there is no significantly peak of absorptance, and $\alpha'_\lambda(d/\lambda)$ is influenced by the period until d equal to 15λ instead of 4λ in the case of $\theta = 1°$.

For structures A-2, the s-polarized absorptance $\alpha'_\lambda(d/\lambda)$ (Fig. 4b'), is similar to that of the related Si-gratings. First, only one of the peaks of the absorptance is significantly important, it is situated at the period $d = 0.76\lambda$, and its magnitude is equal to 0.94 (Fig. 4b'). Second, for a given period d greater than 2λ, the absorptance of the structures A-2 with thickness $h = 0.5\lambda$, at $\theta = 1°$, is greater than that of the related Si-gratings. This effect of filling the trenches of Si-gratings by SiO_2 is already outlined for very thin structures ($h = 0.1\lambda$) but, here, it is more accentuated. At the angle of incidence $\theta = 60°$ the absorptance, of the structures A-2 (Fig. 4b'), is similar to that of the related Si-gratings. Figures $4c$ and $4c'$ show the absorptance, $\alpha'_\lambda(d/\lambda)$, of the structures A-1 and A-2 of the thickness $h = 1\lambda$ at the angles of incidence $\theta = 1°$ and $\theta = 60°$. Analogous behavior of the absorptance versus the period d as in the cases $h = 0.5\lambda$ is observed.

4.2. Effect of the period on p-polarized absorptance at $\theta = 1°$ and $\theta = 60°$

In this subsection we study the influence of the period d on the p-polarized absorptance for the two structures at $\theta = 1°$ and $\theta = 60°$. These two models are with the same filling factor $\varphi = 0.5$. The absorptance is numerically implemented as a function of the period per wavelength $\alpha'_\lambda(d/\lambda)$. The curves of $\alpha'_\lambda(d/\lambda)$ are depicted in figures 5.

For the normal incidence, the p-polarized absorptance of the structure A-1 with thickness $h = 0.1\lambda$ presents an asymptote for d greater than 3.12λ (Fig. 5a). However, an important variation of $\alpha'_\lambda(d/\lambda)$ with the period appeared for d smaller than λ. So, two maxima of the absorptance are observed at $d = 0.25\lambda$ and $d = 0.97\lambda$. A same behavior of the absorptance is outlined at the angle of incidence $\theta = 60°$. In this case the maximum of the absorptance is located at $d = 0.53\lambda$, its magnitude is equal to 0.98. Let's note that the p-polarized absorptance at normal incidence ($\theta = 1°$) is greater than that at $\theta = 60°$, for d belonging the intervals $[0.1\lambda, 0.28\lambda]$ and $[0.85\lambda, 0.98\lambda]$. This behavior is also observed for the second structure but with an increase of the absorptance for the two angles of incidence and all period d (Fig. 5a′).

At the angle of incidence $\theta = 1°$, the absorptance versus the period d oscillates between maxima and minima several times, for each case of model structures A-1 or A-2 having the same thickness $h = 0.5\lambda$ (Fig. 5b, b'). So that, at $\theta = 1°$, three remarkable maxima of the absorptance are observed, both for the Si-gratings and for the related structures A-2. In each model structures case, these maxima are situated at periods d smaller than the wavelength, and their magnitudes are greater than 0.9. Particularly, for the structure A-2 with the period d equal to 0.52λ the absorptance reaches the unity, at $\theta = 1°$ (Fig. 5b′). For this angle of incidence, we note that the asymptotic behavior is established for both structures from d equal to about 6λ.

At the angle of incidence $\theta = 60°$ the p-polarized absorptance of the Si-gratings oscillates versus the period d, until d equal to 8λ (Fig. 5b). Two peaks, of magnitude equal to the unity, are detected at $d = 0.27\lambda$ and $d = 0.42\lambda$. We note that no such a peak appears at $\theta = 1°$ for these gratings with thickness $h = 0.5\lambda$. In addition, at this angle of incidence $\theta = 1°$ the asymptotic behavior is more quickly reached than in the actually case ($\theta = 60°$). Therefore, the existence of the maxima and minima of the absorptance of the Si-gratings persist beyond the period $d = 2.43\lambda$. This effect of the period d on the absorptance is no longer valid when the trenches of the Si-gratings are filled with SiO_2. In fact, figure $5b'$ shows that, for both angles of incidence $\theta = 1°$ and $\theta = 60°$, there is no influence of the period d on the absorptance when d is greater than 6λ. The oscillation already described, in the case A-1 of Si-gratings at $\theta = 60°$, is now drastically attenuated for the related structures in case A-2 (Fig. 5b′). Here again, two structures are perfect absorber, they correspond to the periods $d = 0.26\lambda$ and $d = 0.32\lambda$ (Fig. 5b′). Let's recall that only one analogous structure A-2 has been observed at $\theta = 1°$. For the thickness $h = \lambda$, the absorptance has the same behavior i.e. it has a sinusoidal variation versus the ratio d/λ belonging the intervals $[0.1\lambda, 6\lambda]$ (fig. 5c). The most important difference between those curves and that shown below ($h = 0.5\lambda$) is the increase of the number of peaks and the p-polarized absorptance is equal to the unity for $d = 0.22\lambda$ at $\theta = 1°$ and $\theta = 60°$. Therefore, this Si-grating is a perfect absorber at these two angles of incidence. In addition, at $\theta = 60°$, two other analogous gratings to the latter can be designed for $d = 0.29\lambda$ and $d = 0.36\lambda$. For the structures in case A-2 with the same thickness, $h = \lambda$, and for both angles of incidence,the effect of the period d on the

ISSN 2347-3487
Volume 12 Number 2
Journal of Advances in Physics

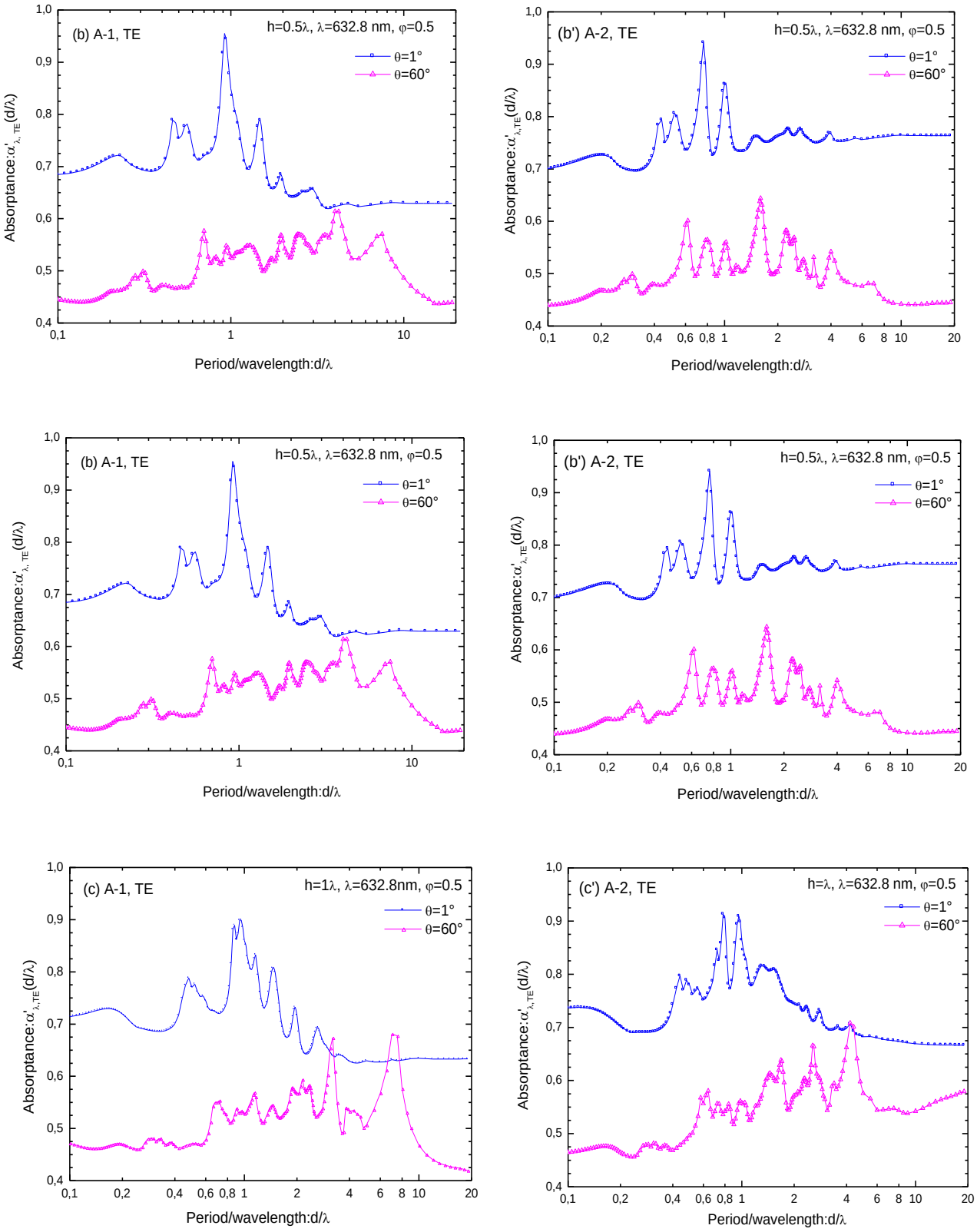

Fig 4. Effect of the period d of structures A-1 and A-2 on the absorptance in the transverse electric polarization case.

ISSN 2347-3487
Volume 12 Number 2
Journal of Advances in Physics

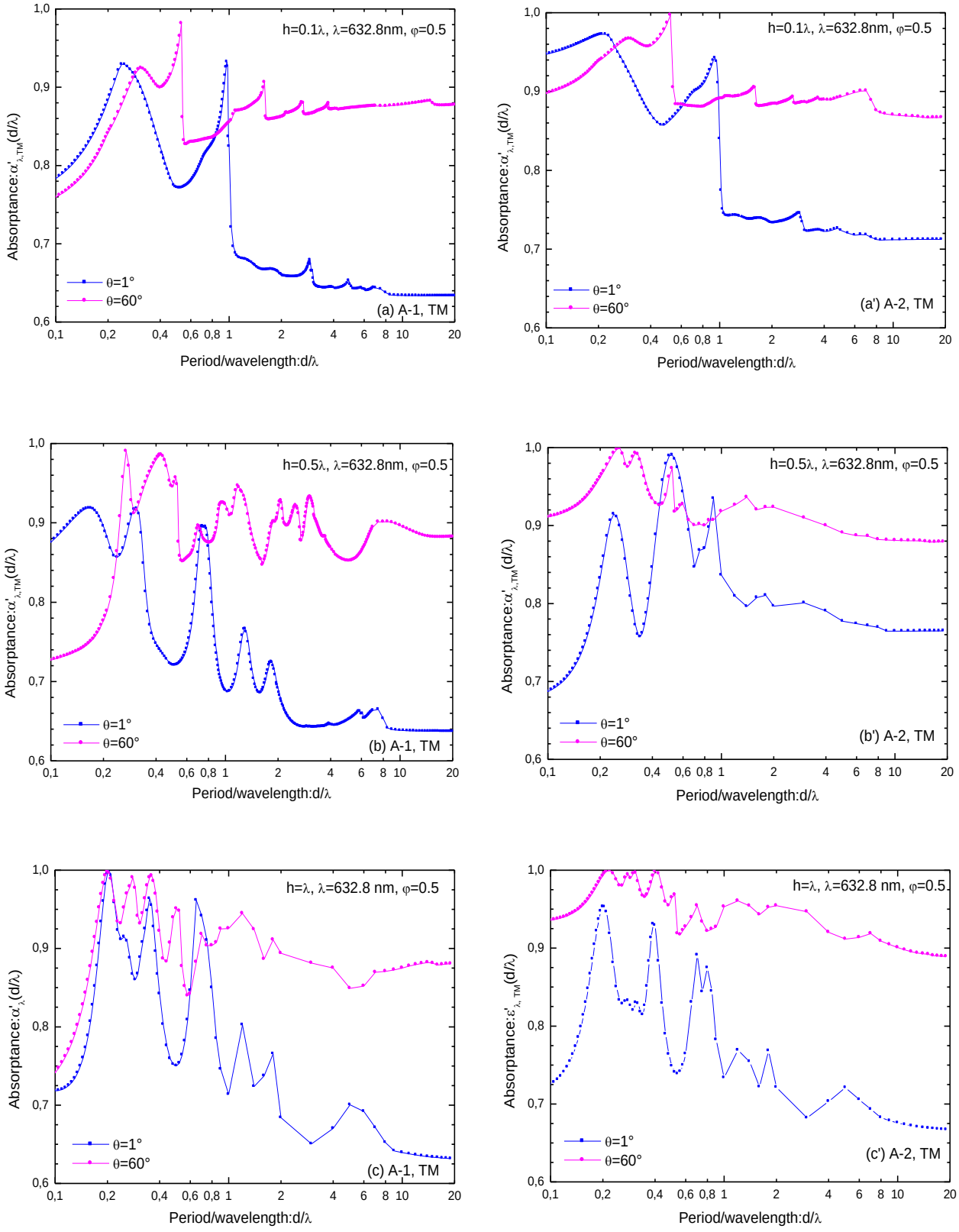

Fig 5. Effect of the period d of structures A-1 and A-2 on the absorptance at the angles of incidence $\theta = 1°$ and $\theta = 60°$ in transverse magnetic polarization case.

absorptance (Fig.5c′) is comparable to that already developed for the similar structures with $h = 0.5\lambda$ (Fig. 5b′). For this structure one clearly detect that the absorptance at $\theta = 60°$ is larger than that determined for $\theta = 1°$ for all period d.

5. CONCLUSION

In this paper the absorptance of two model structures are derived using a Rigorous Coupled Wave Analysis (RCWA). Rectangular grating of silicon (A-1) and an array of SiO_2-filled trenches formed in Si substrate (A-2) are considered. They are characterized by the period d, the thickness h and the filling factor φ. A better comprehension of the radiative behavior of these patterned wafers constitutes our principal goal. This is justified by the wide interest of these model structures because of their various areas of application and their theoretical physics aspects [40-41]. From numerical results presented in this work the following important conclusions can be drawn.

For the Si-rectangular gratings, A-1, with period $d = 2\mu m$ and thickness $h = 0.1\lambda$, the absorptance versus the angle of incidence is not influenced by the filling factor φ both in TE and TM-polarization cases. However, when the trenches of these very thin gratings are filled with SiO_2, the effect of φ is clearly manifested. The absorptance of the structures A-2 is increased with φ in TE-polarization case. But in the TM-polarization case the increase of $\alpha'_\lambda(\theta)$ with φ is limited to $\theta < 60°$; and $\alpha'_\lambda(\theta)$ decreases when φ is increased for θ greater than $60°$. So that, we outline the remarkable intersect point of the curves of TM-polarization absorptance versus θ, $\alpha'_\lambda(\theta)$, for all φ. This point is located at $\theta = 60°$. This implies that structures A-2 characterized by the same period $d = 2\mu m$ and thickness $h = 0.1\lambda$, but with different filling factor φ, have the same absorptance equal to 0.87 at $\theta = 60°$. Analogous influence of φ on the p-polarization absorptance for both structures A-1 and A-2 is also shown when the thickness h is increased to 0.5λ and to λ; the intersection point of the curves $\alpha'_\lambda(\theta)$ is however shifted towards higher values. Therefore, structures A-2 with different filling factor will again be expected to exhibit a same radiative behavior at specific angle of incidence.

The influence of the period d on the absorptance of structures A-1 and A-2 characterized by the same filling factor $\varphi = 0.5$, leads essentially to identify perfect (or nearly perfect) absorber structures of the incident plane wave of wavelength $\lambda = 632{,}8\,nm$. In the s- polarization case at $\theta = 1°$, rectangular Si-gratings, A-1, with thickness $h = 0.5\lambda$ and period $d = 0.92\lambda$ (or $h = \lambda$ and $d = \lambda$) are two examples of these perfect absorbers. Other examples can easily be drawn from figure 4. This is equally true in the TM polarization case (Fig. 5);

REFERENCES

I. J. F. Ody Sacadura: ‘’Influence de la rugosité sur le rayonnement thermique emis par les surfaces opaques: Essai de modèle,’’ J. Int. Heat Mass Transfer 15, 1451 (1972).

II. B. L. Drolen, ‘’Bidirectional reflectance and specularity of twelve spacecraft thermal control materials’’, Journal of Thermophysics and Heat Transfer 6, 672 (1992).

III. M. Laroche, F. Marquier, R. Carminati, J.-J. Greffet, ‘’ Tailoring silicon radiative properties’’, Optics Communications 250, 316 (2005).

IV. B. J. Lee, C. J. Fu, and Z. M. Zhang, ‘’Coherent thermal emission from one-dimensional photonic crystals’’, Appl. Phys. Lett. 87, 071904 (2005).

V. J.-J. Greffet, R. Carminati, K. Joulain, J.-Ph. Mulet, S. Mainguy, Y. Chen,’’Coherent emission of light by thermal sources’’, NATURE 416, 61 (2002).

VI. Y. -B. Chen, Z. M. Zhang, P. J. Timans, ‘’Radiative Properties of Patterned Wafers With Nanoscale Linewidth’’, J. of Heat Transfer 129, 79 (2007).

VII. A. Wirgin, ‘’On Rayleigh's Theory of Partially Reflecting Gratings’’, Optica Acta 28, 1377 (1981).

VIII. J.-J. Greffet, R. Carminati, ‘’Radiative transfer at nanometric scale. Are the usual concepts still valid?’’, Heat and Technology 18, 81 (2000).

IX. K. A. O’Donnell and E. R. Mendez, ‘’Experimental study of scattering from characterized random surfaces’’, J. Opt. Soc. Am. A 4, 1194 (1987).

X. R. A. Dimenna and R. O. Buckius, ‘’Microgeometrical Contour Contributions to Surface Scattering’’ Thermal Sc. & Engin. 2, (1994).

XI. B. K. Sun, X. Zhang and C. P. Grigoropoulost, ‘’Spectral optical functions of silicon in the range of 1.13-4.96 eV at elevated temperatures’’, Int. J. Heat Mass Transfer 40, 1591 (1997).

XII. W. Nakagawa, R.-C Tyan, and Y. Fainman, ‘’Analysis of enhanced second-harmonic generation in periodic nanostructures using modified rigorous coupled-wave analysis in the undepleted-pump approximation’’, J. Opt. Soc. Am. A 19, 1919 (2002).

XIII. J. P. Hugonin, P. Lalanne, I. Delvillar and I. R. Matias, ‘’Fourier modal methods for modeling optical dielectric waveguides’’, Optical and Quantum Electronics 37, 107 (2005).

XIV. L. Del Campo, R. B. Pérez-Sáez, M. J. Tello, X. Esquisabel and I. Fernández, ''Armco Iron Normal Spectral Emissivity Measurements'', Int. J. Of Thermophys. 27, 1160 (2006).

XV. R. A. Dimena, R. O. Buckius, '' Electromagnetic Theory Predictions of the Directional Scattering From Triangular Surfaces'', J. Heat. Transfer 116, 639 (1994).

XVI. D. W. Cohn, K. Tang and R. O. Buckius, ''Comparison of theory and experiments for reflection from microcontoured surfaces'', Int. J. Heat Mass Transfer 40, 3223 (1997).

XVII. J. Liu, S. J. Zhang and Y. S. Chen, ''Rigorous Electromagnetic Modeling of Radiative Interactions with Microstructures Using the Finite Volume Time-Domain Method 1'' Int. J. of Thermophysics 25, 1241 (2004).

XVIII. Q. Huang, Y. Yu and J. Yu, ''Design and realization of a microracetrack resonator based polarization splitter in silicon-on-insulator'', J. Opt. A: Pure Appl. Opt. 11, 015506 (2009).

XIX. A. Sentenac and J.-J. Greffet, '' Mean-field theory of light scattering by one-dimensional rough surfaces'', J. Opt. Soc. Am. A 15, 528 (1998).

XX. D. L. C. Chan, M. Soljacic and J. D. Joannopoulos, '' Thermal emission and design in 2D-periodic metallic photonic crystal slabs'', Opt. Express 14, 8785 (2006).

XXI. E. I. Thorsos, '' The validity of the Kirchhoff approximation for rough surface scattering using a Gaussian roughness spectrum'', J. Acoustic .Soc. Am. 83, 78 (1988).

XXII. E. Popov, S. Enokh, G. Tayeb, M. Nevière, B. Gralak and N. Bonod, '' Enhanced transmission due to nonplasmon resonances in one- and two-dimensional gratings'', Appl. Opt. 43, 999 (2004).

XXIII. M.-K. Seo, J.-K. Yang, K.-Y. Jeong, H.-G. Park, F. Qian, H.-S. Ee, Y.-S. No, and Y.-H. Lee, ''Modal Characteristics in a Single-Nanowire Cavity with a Triangular Cross Section'', Nano Lett. 8, 4534 (2008).

XXIV. S. H. Zaidi, A.-S. Chu and S. R. J. Brueck, "Opitcal-Properties of Nanoscale, One-Dimensional Silicon Grating Structures", J. Appl. Phys. 80, 6997 (1996).

XXV. I. Celanovic, F. OSullivan, N. Jovanovic, M. Qi, J.G. Kassakian ,''1D and 2D photonic crystals for thermophotovoltaic applications'', Proceedings of SPIE - The International Society of Optical Engineering (2004).

XXVI. M. G. Moharem and T. K. Gaylord, ''Diffraction analysis of dielectric surface-relief gratings'', J. Opt. Soc. Am. 72, 1385 (1982).

XXVII. N. Chateau and J.-P. Hugonin, ''Algorithm for the rigorous coupled-wave analysis of grating diffraction'', J. Opt. Soc. Am. A 11, 1321 (1994).

XXVIII. L. Li and C. W. Haggans, '' Convergence of the coupled-wave method for metallic lamellar diffraction gratings'', J. Opt. Soc. Am. A 10, 1184 (1993).

XXIX. L. Li, ''Use of Fourier series in the analysis of discontinuous periodic structures'', J. Opt. Soc. Am. A 13, 1870 (1996).

XXX. L. Li, '' Formulation and comparison of two recursive matrix algorithms for modeling layered diffraction gratings'', J. Opt. Soc. Am. A 13, 1024 (1996).

XXXI. F. Ghmari, T. Ghbara, M. Laroche, R. Carminati, J.-J. Greffet, '' Influence of microroughness on emissivity'', J. App. Phys. 96, 2656 (2004).

XXXII. K. Tang, R. Dimena, R. O. Buckius, ''Regions of validity of the geometric optics approximation for angular scattering from very rough surfaces'', Int. J. Heat Mass Transfer 40, 49, (1996).

XXXIII. A. A. Maradudin and T. Michel, A.R McGurn and E.R Méndez, '' Enhanced backscattering of light from a random grating'', Annals of Physics 203, 2, (1990).

XXXIV. J. A. Sanchez-Gil and M. Nieto-Vesperinas, '' Light scattering from random rough dielectric surfaces'', J. Opt. Soc. Am. A 8, 1270 (1991).

XXXV. F. Ghmari, I. Sassi, M. S. Sifaoui, ''Directional hemispherical radiative properties of random dielectric rough surfaces'', Waves in Random and Complex Media 15, 469 (2005).

XXXVI. M. F. Modest, ''Radiative heat Transfer'', Second Edition, ACADEMIC PRESS (2003).

XXXVII. W. AiHua and C. JiuJu, '' Modeling radiative properties of nanoscale patterned wafers'', Sci. China Tech. Sci. 53, 352 (2010).

XXXVIII. J. Qiu, L.H.Liu, P.-f. Hsu, ''Radiative properties of optical board embedded with optical black holes'' J. of Quantitative Spectroscopy and Radiative Transfer 112, 832 (2011).

XXXIX. T. K. Gaylord and M. G. Moharam, ''Planar dielectric grating diffraction theories'', Applied Physics B, 28, 1 (1982).

XL. X. Xiong, Z.-H. Xue, C. Meng, S.-C. Jiang, Y.-H. Hu, R.-W. Peng, and M. Wang, "Polarization-dependent perfect absorbers/reflectors based on a three-dimensional metamaterial" PHYSICAL REVIEW B 88, 115105 (2013).

XLI. N. Dahan, Z. Jehl, J. F. Guillemoles, D. Lincot, N. Naghavi, and J.-J. Greffet "Using radiative transfer equation to model absorption by thin Cu(In,Ga)Se2 solar cells with Lambertian back reflector", OPTICS EXPRESS 21, 2563 (2013).